# Photoelectron Diffraction Mapping: Molecules Illuminated from Within

A. Landers,[1,*] Th. Weber,[2] I. Ali,[3] A. Cassimi,[4] M. Hattass,[2] O. Jagutzki,[2] A. Nauert,[2] T. Osipov,[3] A. Staudte,[2,5] M. H. Prior,[5] H. Schmidt-Böcking,[2] C. L. Cocke,[3] and R. Dörner[6]

[1]*Department of Physics, Western Michigan University, Kalamazoo, Michigan 49008*
[2]*Institut für Kernphysik, University of Frankfurt, August-Euler Strasse 6, D-60486 Frankfurt, Germany*
[3]*Department of Physics, Kansas State University, Cardwell Hall, Manhattan, Kansas 66506*
[4]*CIRIL/CEA/CNRS/ISMRA, Université de Caen, Box 5133, F-14070 Caen Cedex 5, France*
[5]*Chemical Sciences Division, Lawrence Berkeley National Laboratory, Berkeley, California 94720*
[6]*Fakultät für Physik, University of Freiburg, Hermann Herderstrasse 3, D-79104 Freiburg, Germany*

We demonstrate the use of a multiparticle coincidence technique to image the diffraction of an electron wave whose source is placed at a specific site in a free molecule. Core-level photoelectrons are used to illuminate the molecule from within. By measuring the vector momenta of two molecular fragments and the photoelectron, a richly structured electron diffraction pattern is obtained in a body-fixed frame of the randomly oriented molecule in the gas phase. We illustrate this technique for CO, creating a photoelectron from the $C(1s)$ shell and scanning its energy from zero to 30 eV.

PACS numbers: 33.80.Eh, 33.90.+h

The scattering and diffraction of x rays and electrons has long been a tool for exploration of the structure and properties of matter. In the case of electrons, two prominent examples are the electron microscope which uses the diffraction of fast electrons and the discovery of the quark by relativistic electron scattering. In this Letter we present the first comprehensive images of photoelectron diffraction by a molecule in the gas phase. The probe electron wave is created inside a carbon monoxide molecule when a photoelectron is released from the carbon $K$ shell by absorption of an x ray. Similar x-ray photoelectron diffraction (XPD) techniques have previously been possible only in crystals [1] and absorbates [2], where they have provided information on physical properties such as the positions of nearest neighbors. For free molecules in the gas phase, XPD can be fully utilized only if the molecules can be oriented in space. In this Letter we demonstrate a three-dimensional multiparticle imaging technique, which determines the coincident vector momenta of the photoelectron and all molecular fragments with $4\pi$ solid-angle coverage.

Core-level photoelectron emission from spatially oriented molecules poses a formidable challenge to quantum mechanical theory. In atomic photoionization, single photoelectron angular distributions have trivial structure fully described with one parameter [3]. For molecular species, however, a far more complex structure was predicted in 1975 by Dehmer and Dill [4] and subsequently observed experimentally [5]. Here the electron wave propagates through the nonspherical potential of the molecule and, via coupling to the nuclear motion, may emerge with any value of angular momentum in the asymptotic continuum. In a multiple scattering picture, the intensity in a given direction with respect to the molecular frame results from the addition of a direct wave, from the $K$ shell of the ionized atom, with waves scattered one or more times from the other atoms in the molecule. These effects can also

lead to an enhancement of the absorption cross section for a range of photon energies, commonly known as a shape resonance [4]. The angular distributions of the photoelectrons in the region of such shape resonances have been studied in a number of pioneering experiments [5,7].

The photoionization/dissociation of CO above the carbon $K$ edge is a multistep process beginning with the promotion of the $C(1s)$ electron to the continuum where it interacts with the two-center potential as it exits the molecule. The ejected photoelectron wave is a signature of the molecular potential and is the focus of this Letter. The electron emission is promptly followed by the decay of the excited $CO^{+*}$ molecule, primarily through autoionization channels, leading to the dissociation of the molecular ion. In order to fully observe the rich structure of the continuum electron wave in the molecular potential, knowledge of the orientation of the molecular axis is required. Determining the axis *a posteriori* requires that the axial recoil approximation be valid [6]. That is, the dissociation time of the molecule must be substantially shorter than the characteristic period of rotation, so that the fragments are ejected along the internuclear axis of the molecule, and the autoionization must occur before the molecule rotates away from its orientation at the time of photoionization. Measurement of one (or both) of the fragment momentum vectors then determines the orientation of the internuclear axis. Two techniques based on this concept have been employed previously for measuring angle-resolved photoelectron-photoion coincidences. The first was by Shigemasa *et al.* in 1995, who used two parallel plate analyzers, one each for the photoelectron and a coincident fragment ion [5]. By varying the relative angle between the analyzers, they were able to reconstruct angular distributions of photoelectrons from fixed-in-space molecules. The second was by Heiser *et al.* who used a time-of-flight electron spectrometer and pulsed extraction

of a coincident fragment ion to a position sensitive detector [8]. This technique yielded measurements of photoelectrons for all orientations of the molecule relative to the photon polarization vector but was limited to the specific angles chosen for the electron analyzers.

In this Letter, we present a method which produces a complete image of the emitted photoelectron wave from $K$-shell photoionization of spatially oriented molecules, without any restrictions on the emission angles of the electron or molecular fragments. The technique is based on cold target recoil ion momentum spectroscopy [9] and is similar to the one used by Lafosse *et al.* for the study of valence band photoemission [10]. We have measured, for each event, the direction and energy of the two ion fragments and the full momentum vector of the $C(1s)$ photoelectron from the photoionization of CO by linearly polarized photons with energies from 294 to 326 eV. This energy range encompasses the threshold of $C(1s)$ photoionization and the $\sigma$ shape resonance near 10.2 eV above the carbon $K$ edge. Because the photon and electron binding energies are known, we are able to distinguish the $C(1s)$ electrons from any other electrons (e.g., Auger) that are detected. This multiparticle imaging technique has several advantages over previous experiments. First, the electrons are measured with $4\pi$ solid-angle coverage, so that the angular distributions relative to the internuclear axis, photon polarization, and propagation vectors are measured simultaneously. Second, both molecular fragments are measured so that the preionization orientation of the molecule is obtained as well as the kinetic energy release and the charge states of the final fragments. This permits the exploration of a number of phenomena such as the dependence of the electron emission on the kinetic release and the validity of the axial recoil approximation. We must, however, confine the focus of this Letter to the photoelectron emission for oriented molecules and present additional details in future work. Third, and finally, the full solid angle yields the high coincidence count rate required for highly differential measurements.

Our experiments were performed at beam line 9.3.2 at the Advanced Light Source at Lawrence Berkeley National Laboratory. A molecular beam of CO was intersected at $90°$ with the photon beam to form a localized interaction volume. All ions and electrons created in this volume were accelerated by a static electric field towards two position-sensitive detectors, which were equipped with multihit delay-line anodes [11]. The associated times of flight were then measured relative to the interaction (photon bunch) time. A magnetic field confined the electrons to a helical trajectory, ensuring $4\pi$ solid angle coverage for kinetic energies up to 30 eV [12]. From this information, the complete coincident vector momenta of the photoelectron and fragment ions were then reconstructed. The abundant statistics due to the large solid angle allowed the photon energy to be scanned by 100 meV steps over a range from 0 to 30 eV above the carbon $1s$ threshold. By recording the photon energy as an additional parameter, we were able to

extract the photoelectron diffraction pattern over a range of electron energies.

Figure 1 shows momentum distributions of the photoelectrons from the $K$ shell of the carbon atoms in oriented CO molecules. The images are presented in the laboratory frame with the respective horizontal and vertical axes defined by the linear polarization and propagation vectors of the photon. The individual images 1a–1c correspond to particular orientations of the molecule relative to the polarization vector. The photoelectron energy is displayed through the radial size of the momentum vector; the circular edge of each image is therefore determined by the 30 eV (1.5 a.u. momentum) upper bound of the photon energy range. The angular momentum character of the outgoing wave can be seen in the polar distributions of this vector. The intensity of the images, representing the square of the amplitude for the bound $\rightarrow$ continuum transitions, is indicated by the color legend shown in the figure. Figure 1a shows the image corresponding to the $1s\sigma \rightarrow \varepsilon l\sigma$ transition (molecular axis parallel to polarization vector). This comprehensive picture makes immediately evident the $f$-wave resonance of the scattered wave in the molecular potential at a momentum near 0.8 a.u. (dashed circle) and displays the higher angular momenta populated on the resonance through the characteristic side lobes in the pattern. The greater strength of the resonant wave emitted along the molecular axis toward the right is caused by interference of the direct wave from the carbon source with that scattered from the oxygen partner. From the same measurement we generate momentum maps for other alignments of the molecule. Figure 1b shows the photoelectron image for the $1s\sigma \rightarrow \varepsilon l\pi$ (molecular axis perpendicular to polarization vector) transition. Because the molecule does not resonate nearly as strongly in this orientation, the contribution from high angular momentum components is much less pronounced. The photoelectron distribution for molecules oriented at $45°$ to the polarization vector is shown in Fig. 1c. As described in more detail below, this distribution results from a coherent superposition of the amplitudes for $\sigma$ and $\pi$ transitions shown in 1a and 1b. We present the continuous evolution of these images as the molecule rotates relative to the polarization vector in an animation that is available in the on-line version of this journal. These pictures are the molecular analog of the most advanced XPD technology in solid state physics [2], and they are a unique fingerprint of the molecular potential.

As recently described by Ito *et al.*, measurement of all the amplitudes and relative phases for the bound-to-continuum transitions constitutes a so-called "quantum mechanically complete" experiment [14]. Figures 2a and 2d show the results for $C(1s)$ photoelectrons ($\sigma$ and $\pi$ transitions, respectively) produced at 10.4 eV above the carbon $K$ edge. This energy is near the peak in the $\sigma$ resonance and corresponds to the dashed circles in Fig. 1. These data are in agreement with those presented by Shigemasa *et al.* [15] and Motoki *et al.* [16]. Since

our data set is comprehensive, it includes all other relative orientations of the molecule and the polarization vector as well; some additional orientations are shown in Figs. 2b and 2c. In some cases we can extract the contributions of different partial waves to the continuum photoelectron wave by fitting the experimental angular



distributions by coherent sums of the spherical harmonics $Y_{l0}$ (for the $1s\sigma \rightarrow \varepsilon l\sigma$ transition) or $Y_{l\pm1}$ (for the $1s\sigma \rightarrow \varepsilon l\pi$ transition). The angular distributions for any given molecular orientation can be represented by a linear combination of the $\sigma$ and $\pi$ amplitudes. The curves in Figs. 2a–2d are derived from a fit to the partial wave expansion as described in [17], where we have optimized, by least squares adjustment, the (complex) amplitudes for $l = 0$–$4$, $m = 0$ for the parallel and $l = 1$–$4$, $m = \pm1$ for the perpendicular transitions. From symmetry, the amplitudes for $m = 1$ and $m = -1$ for any given $l$ must be equal. Since each amplitude is complex, this results in a total of 17 free independent parameters in the following fit function:

$$F(\phi_e, \theta_e, \theta_\varepsilon) = \left| \left( \sum_{l=0,\ldots,4,\, m=0} A_{lm} Y_{lm}(\phi_e, \theta_e) \cos(\theta_\varepsilon) \right. \right.$$

$$+ \sum_{l=1,\ldots,4,\, m=-1,1} A_{lm} Y_{lm}(\phi_e, \theta_e)$$

$$\left. \left. \times \sin(\theta_\epsilon) \right)^2 \right|, \tag{1}$$

where $\theta_e$ and $\phi_e$ are the emission angles of the electron in the molecule frame and $\theta_\varepsilon$ is the angle of the polarization vector relative to the molecule. $F$ is then the intensity of emission into a differential solid angle located at $\theta_e$, $\phi_e$, in a coordinate system with the polarization vector along the $z$ axis. Figure 2 shows only a few selected angles, but the fit has been performed on our entire data set, making use of the statistics at all angles. The high fidelity of the fitted curves to the data shown in Fig. 2 demonstrates that the phase relations can be successfully extracted from our data. (The details of this fit as well as complex amplitudes will be presented in a future paper.) Therefore, from a quantum mechanical point of view, this becomes, within the truncated number of $l$'s, a complete experiment. The pioneering experiments in Ref. [7] were performed with two molecular orientations (parallel and perpendicular to
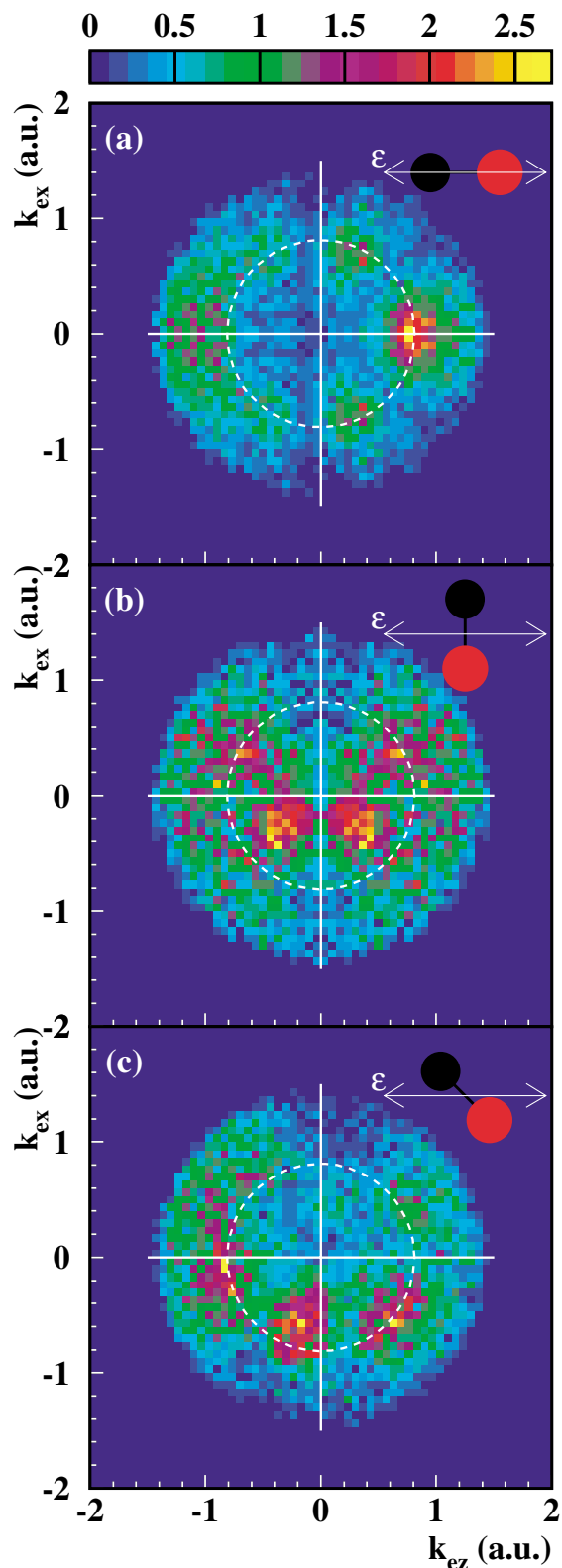
FIG. 1 (color). The momentum distribution of C$(1s)$ electrons emitted from a CO molecule for three different orientations of the molecule (C black, O red) relative to the photon linear polarization $\varepsilon$. The axes are defined by the photon linear polarization (horizontal) and propagation vector (vertical, down). The angular distribution for a fixed electron energy $E$ (a.u.) is given by the intensity variation along a circle centered at the origin with radius equal to $(2E)^{1/2}$. The electron energy was scanned from 0 to 1.1 a.u. (0–30 eV) in steps of 100 meV. Intensity, i.e., the relative transition probability, is represented by the color scale at the top. (a) $1s\sigma \rightarrow \varepsilon l\sigma$ transition: $\varepsilon$ parallel to the molecular axis. The onset and decline of the strong angular variations in intensity at the resonance energy (shown along the dashed circle) are indicative of the coupling to higher angular momenta in the shape resonance region. (b) $1s\sigma \rightarrow \varepsilon l\pi$ transition: $\varepsilon$ perpendicular to the molecular axis. In this case, the coupling to higher angular momenta is much less pronounced than in (a). (c) $\varepsilon$ is at 45° to the molecule. An animated version of these frames showing their evolution as the molecule is rotated is available in the on-line version of this journal.
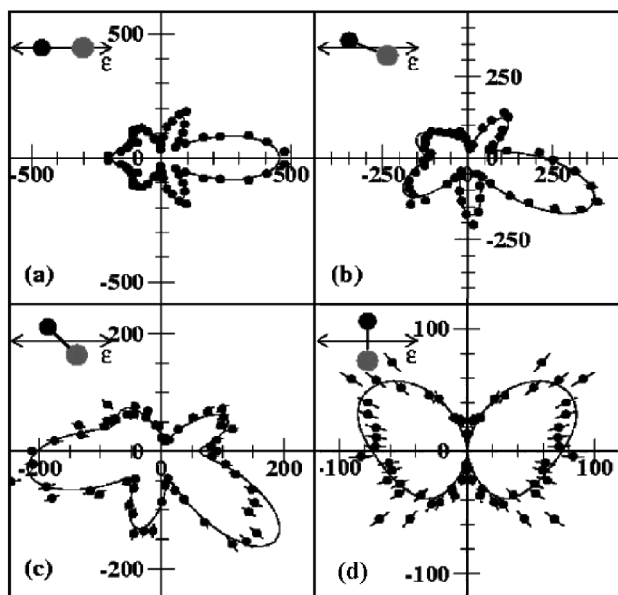
FIG. 2. Polar distributions of 10.2 eV photoelectrons in the frame of the incident photon corresponding to the dashed circles in Fig. 1. The schematic in the upper left corner of each frame shows the orientation of the molecule (grey oxygen, black carbon) relative to the photon polarization vector (arrow). The black circles are the measurements and the solid curves represent the fit to the spherical harmonic expansion [see Eq. (1)]. (a) and (d) show angular distributions for the $1s\sigma \to \varepsilon l\sigma$ and $1s\sigma \to \varepsilon l\pi$ transitions, respectively. (b) and (c) show distributions for intermediate angles. The large change in scale between (a) and (d) reflects the predominance of the $1s\sigma \to \varepsilon l\sigma$ transition, (a). An animated version of this figure, showing all polarization angles, can be found in the on-line version of this journal.

the polarization vector), and hence the relative phase between the $\sigma$ and $\pi$ amplitudes could not be extracted. The continuous evolution of the angular distribution from the parallel to the perpendicular orientation of the molecule can be viewed in an animated version of Fig. 2 in the on-line version of this journal.

In addition to the orientation information, we determine the final charge state and the kinetic energy released in the dissociation, which combine to give a signature of the dissociative state of the molecular ion. It is thus possible to investigate the degree of correlation between the photoelectron emission pattern and the final states of the molecular ion, a rather detailed description of the behavior of these complex systems. This can be a critical factor in the ability to observe photoelectron diffraction patterns shown above.

The topographical nature of the photoelectron momentum images gives at once an informative and illuminating vista of photoemission in the shape resonance regime. These emission patterns reflect the electron wave propagation in the full three-dimensional potentials of the molecule. One possible future application of the approach described here is its use as a time delayed probe for photochemical reactions triggered by short laser pulses. This would provide a unique tool to obtain temporally and spatially resolved "snapshots" of the evolution of intramolecu-

lar potentials and molecular structure. This technique has proven to be quite effective for simple diatomic molecules. However, it becomes increasingly difficult to take advantage of the axial recoil approximation as molecules of interest become more complex. Possible solutions include measurement of three or more molecule fragments and "tagging" a molecule with a single atom with an isolated $K$ edge.

*Electronic address: allen.landers@wmich.edu

[1] C. S. Fadley, Prog. Surf. Sci. **16**, 275 (1984).
[2] S. H. Xu, M. Keeffe, Y. Yang, C. Chen, M. Yu, G. J. Lapeyre, E. Rotenberg, J. Denlinger, and J. T. Yates, Jr., Phys. Rev. Lett. **84**, 939 (2000).
[3] V. Schmidt, *Electron Spectrometry of Atoms Using Synchrotron Radiation* (Cambridge University Press, Cambridge, 1997).
[4] J. L. Dehmer and D. Dill, Phys. Rev. Lett. **35**, 213 (1975).
[5] E. Shigemasa, J. Adachi, and M. Oura, and A. Yagishita, Phys. Rev. Lett. **74**, 359 (1995).
[6] R. Zare, Mol. Photochem. **4**, 1 (1972).
[7] E. Shigemasa, J. Electron Spectrosc. Relat. Phenom. **88–91**, 9 (1998).
[8] F. Heiser, O. Gessner, J. Viefhaus, K. Wieliczek, R. Hentges, and U. Becker, Phys. Rev. Lett. **79**, 2435 (1997).
[9] R. Dorner *et al.,* Phys. Rep. **330**, 95 (2000).
[10] A. Lafosse, M. Lebech, J. C. Brenot, P. M. Guyon, O. Jagutzki, L. Spielberger, M. Vervloet, J. C. Houver, and D. Dowek, Phys. Rev. Lett. **84**, 5987 (2000).
[11] Roentdek GmbH (www.Roentdek.com).
[12] R. Moshammer *et al.,* Nucl. Instrum. Methods Phys. Res., Sect. B **108**, 425 (1996).
[13] E. Shigemasa, T. Hayaishi, T. Sasaki, and A. Yagishita, Phys. Rev. A **47**, 1824 (1993).
[14] K. Ito, J. Adachi, Y. Hikosaka, S. Motoki, K. Soejima, A. Yagishita, G. Raseev, and N. A. Cherepkov, Phys. Rev. Lett. **85**, 46 (2000).
[15] E. Shigemasa, J. Adachi, K. Soejima, N. Watanabe, A. Yagishita, and N. A. Cherepkov, Phys. Rev. Lett. **80**, 1622 (1998).
[16] S. Motoki, J. Adachi, Y. Hikosaka, K. Ito, M. Sano, K. Soejima, A. Yagishita, G. Raseev, and N. A. Cherepkov, J. Phys. B **33**, 4193 (2000).
[17] N. A. Cherepkov, G. Raseev, J. Adachi, Y. Hikosaka, K. Ito, S. Motoki, M. Sano, K. Soejima, and A. Yagishita, J. Phys. B **33**, 4213 (2000).